

## The kinetics for ammonium and nitrite oxidation under the effect of hydroxylamine

Xinyu Wan, Pengying Xiao, Daijun Zhang, Peili Lu, Zongbao Yao and Qiang He

### ABSTRACT

The kinetics for ammonium ( $\text{NH}_4^+$ ) oxidation and nitrite ( $\text{NO}_2^-$ ) oxidation under the effect of hydroxylamine ( $\text{NH}_2\text{OH}$ ) were studied by respirometry using the nitrifying sludge from a laboratory-scale sequencing batch reactor. Modified models were used to estimate kinetics parameters of ammonia and nitrite oxidation under the effect of hydroxylamine. An inhibition effect of hydroxylamine on the ammonia oxidation was observed under different hydroxylamine concentration levels. The self-inhibition coefficient of hydroxylamine oxidation and noncompetitive inhibition coefficient of hydroxylamine for nitrite oxidation was estimated by simulating exogenous oxygen-uptake rate profiles, respectively. The inhibitive effect of  $\text{NH}_2\text{OH}$  on nitrite-oxidizing bacteria was stronger than on ammonia-oxidizing bacteria. This work could provide fundamental data for the kinetic investigation of the nitrification process.

**Key words** | aerobic ammonium oxidation, hydroxylamine, inhibition kinetics, nitrite oxidation, parameter estimation

**Daijun Zhang**  
**Peili Lu**

State Key Laboratory of Coal Mine Disaster Dynamics and Control, Chongqing University, Chongqing 400030, China

**Xinyu Wan**  
**Pengying Xiao**

**Daijun Zhang** (corresponding author)

**Peili Lu**

**Zongbao Yao**

Department of Environmental Science, Chongqing University, Chongqing 400030, China  
E-mail: dzhang@cqu.edu.cn

**Pengying Xiao**

School of Chemical Engineering, Chongqing University of Technology, Chongqing 400054, China

**Qiang He**

Key Laboratory of Three Gorges Reservoir Region's Eco-environment, Ministry of Education, Chongqing University, Chongqing 400030, China

### INTRODUCTION

Nitrification consists of ammonium oxidation to nitrite by ammonia-oxidizing bacteria (AOB) and further  $\text{NO}_2^-$  oxidation to  $\text{NO}_3^-$  by nitrite-oxidizing bacteria (NOB). In  $\text{NH}_4^+$  oxidation step, ammonia is first oxidized to hydroxylamine under the catalysis of ammonia monooxygenase (AMO) and then is oxidized to nitrite catalyzed by hydroxylamine oxidoreductase. Hydroxylamine serves as a biodegradable intermediate in this two-step process (Hoffman & Lees 1953). The oxidation of  $\text{NH}_2\text{OH}$  provides the energy and electrons for the oxidation of ammonia. The electrons generated in the  $\text{NH}_2\text{OH}$  oxidation are partially channeled to oxygen, the terminal electron acceptor, and partially back to AMO (Hooper *et al.* 1997) for the regeneration of  $\text{NH}_2\text{OH}$ . However, the oxidation of  $\text{NO}_2^-$  to nitrate is an independent process compared with the oxidation of  $\text{NH}_4^+$  in nitrification. Although nitrifiers and nitrification are known to be affected by hydroxylamine, the mechanism of hydroxylamine affect in nitrification is still ambiguous (Harper *et al.* 2009). Therefore, the study of nitrification in

engineered and natural systems should include close attention to  $\text{NH}_2\text{OH}$  dynamics in order to avoid misinterpretations.

The activated sludge models (ASM1, ASM2 and ASM3) (Henze *et al.* 2006), published by the International Water Association, are widely accepted by both the scientific community and practitioners for the modeling of wastewater treatment processes. Bing-Jie Ni (Ni *et al.* 2014) also suggested a model, introducing reduced mediator (Mred) and oxidized mediator (Mox) as new components to link the electron transfer from oxidation to reduction, to describe the ammonia oxidation process. However,  $\text{NH}_2\text{OH}$  and the effects of these have not been considered in the above models. This could consequently result in meaningless parameter estimates describe in autotrophic ammonia oxidation.

This study aimed at investigating  $\text{NH}_4^+$  oxidation and  $\text{NO}_2^-$  oxidation under the external addition of hydroxylamine. A modified model was proposed to stimulate the kinetics of nitrification. The oxygen-uptake rate (OUR)

measured through respirometry was used to estimate the kinetic parameters. The results will contribute to understanding of the effect of hydroxylamine on the nitrification.

## MATERIALS AND METHODS

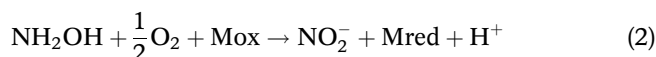
### Nitrifying culture

A nitrifying enrichment consortium was grown and maintained in two 4-L sequencing batch reactors (SBRs). The reactors were operated with a 240 min cycle, consisting of 210 min stirring and 12 min feeding, 18 min of settling and 12 min decanting. The mixed liquor volatile suspended solids (MLVSS) concentration of the SBR was maintained at approximately  $1.3 \pm 0.05$  g/L with a sludge retention time of 20 days. A total of 2 L of synthetic wastewater was fed every cycle with the ammonium (in the form of  $(\text{NH}_4)_2\text{SO}_4$ ) concentration of 200 mg-N/L. The composition of the synthetic wastewater was (units are expressed in g/L except for the micro-amount element solution):  $\text{KaH}_2\text{PO}_4$  0.175,  $\text{NaHCO}_3$  2.6,  $\text{CaCl}_2 \cdot 2\text{H}_2\text{O}$  0.3,  $\text{MgSO}_4 \cdot 7\text{H}_2\text{O}$  0.3,  $\text{NaHCO}_3$  2.6,  $\text{FeSO}_4$  0.00625, EDTA 0.00625 and 1 mL/L of micro-amount elements solution. The micro-amount element solution consisted of (g/L): EDTA 15,  $\text{H}_3\text{BO}_4$  0.014,  $\text{MnCl}_2 \cdot 4\text{H}_2\text{O}$  0.99,  $\text{CuSO}_4 \cdot 5\text{H}_2\text{O}$  0.25,  $\text{ZnSO}_4 \cdot 7\text{H}_2\text{O}$  0.43,  $\text{NiCl}_2 \cdot 6\text{H}_2\text{O}$  0.19,  $\text{Na}_2\text{SeO}_4 \cdot 10\text{H}_2\text{O}$  0.21, and  $\text{Na}_2\text{MoO}_4 \cdot 2\text{H}_2\text{O}$  0.22. The pH of the influent was always kept in the range  $7.5 \pm 0.1$  by dosing hydrochloric acid. The temperature of the reactors was maintained at  $25 \pm 1^\circ\text{C}$  using a water bath.

### Kinetic models for $\text{NH}_4^+$ and $\text{NO}_2^-$ oxidation under the effect of $\text{NH}_2\text{OH}$

To model the ammonia oxidation process in this study, the model suggested by Bing-Jie Ni was simplified with Mred (reduced form of the electron carriers) and Mox (oxidized form of the electron carriers) transferring electrons between ammonium oxidation and hydroxylamine oxidation process (Equations (1) and (2)). This simplified model concentrates on the  $\text{NH}_4^+$ -N oxidation step and  $\text{NH}_2\text{OH}$  oxidation step without considering the gas emissions. The simplification is accessible because ammonium was seldom emitted as nitrous oxide (about 2.8%) or nitric oxide (negligible) during stable ammonia oxidation (Kampschreur *et al.* 2007). A Haldane-type inhibition term  $S_{\text{NH}_2\text{OH}} / (K_{\text{NH}_2\text{OH}} + S_{\text{NH}_2\text{OH}} + (S_{\text{NH}_2\text{OH}})^2 / K_{\text{NH}_2\text{OH},I})$ , with  $K_{\text{NH}_2\text{OH},I}$  being an extra parameter, was applied for

the hydroxylamine oxidation step since the experiment data from the respirometer demonstrated a self-inhibition effect of hydroxylamine.



The interconversion between Mred and Mox is modeled by an increase in Mred being balanced by a decrease in Mox and vice versa ( $\text{Mred} \rightleftharpoons \text{Mox} + 2\text{e}^- + 2\text{H}^+$ ), with the total level of electron ( $C_{\text{tot}}$ ) being held as constant ( $S_{\text{Mred}} + S_{\text{Mox}} = C_{\text{tot}}$ ).

As  $\text{NH}_2\text{OH}$  is not the substrate of NOB, a noncompetitive inhibition model was applied to modeling the nitrite oxidation process in NOB under the influence of  $\text{NH}_2\text{OH}$ . The total kinetics and stoichiometry of the above model are summarized in Table 1. Model simulating for all kinetic parameter estimates were carried out with AQUASIM software (Reichert 1998). Initial concentration of substrates and biomass, OUR data and several cited parameters were input as the original data of the modeling process. All the parameters including the estimated and cited ones were listed and are indicated in Table 3.

### Respirometric tests

Nitrifying cultures were withdrawn from the SBR just before the end of the reaction cycle and washed three times in ammonia-free feed medium. The washed cell suspensions were oxygenated with pure oxygen gas for 5 min and then added to the respirometer. All the respirometric tests were carried out in triplicate at a temperature of  $25^\circ\text{C}$  and a pH of  $7.5 \pm 0.1$  via an extent integrated hybrid respirometer (Peili *et al.* 2006). Briefly, the nitrifying sludge was pumped by a peristaltic pump (Baoding Longer, BT00-600M) to circulate between the two chambers. The large chamber with work volume 4 L was an aeration vessel equipped with porous distributor while the respiration chamber with work volume 1 L was not aerated and completely closed. The dissolved oxygen (DO) concentration in the effluent and influent of the respiration chamber was measured by two DO electrodes (Mettler Toledo Inpro6800). The electrodes were connected to a transmitter (Mettler Toledo, O24100e) that was, in turn, connected to a computer via a data-acquisition interface. After a 10-minute-period of endogenous activity, respirometric assays were initiated by spiking the biomass with appropriate substrates (ammonia or hydroxylamine). Software based on LabVIEW

**Table 1** | Stoichiometry and process kinetics for  $\text{NH}_4^+$  and  $\text{NO}_2^-$  oxidation

	$S_{\text{O}_2}$	$S_{\text{NH}_3}$	$S_{\text{NH}_2\text{OH}}$	$S_{\text{NO}_2}$	$S_{\text{NO}_3}$	$S_{\text{Mred}}$	$S_{\text{Mox}}$	Rate
AOH	-1	-1	1			-1	1	$R_{\text{NH}_4^+} \frac{S_{\text{NH}_4^+}}{K_{\text{NH}_4^+} + S_{\text{NH}_4^+}} \frac{S_{\text{Mred}}}{K_{\text{Mred}} + S_{\text{Mred}}} X_{\text{AOB}}$
HON	$-\frac{1}{2}$		-1	1		1	-1	$R_{\text{NH}_2\text{OH}} \frac{S_{\text{NH}_2\text{OH}}}{K_{\text{NH}_2\text{OH}} + S_{\text{NH}_2\text{OH}} + \frac{(S_{\text{NH}_2\text{OH}})^2}{K_{\text{NH}_2\text{OH},I}}} \frac{S_{\text{Mox}}}{K_{\text{Mox}} + S_{\text{Mox}}} X_{\text{AOB}}$
NO	$-\frac{1}{2}$			-1	1			$\frac{R_{\text{NO}_2^-}}{\left(1 + \frac{S_{\text{NH}_2\text{OH}}}{K_{\text{NO}_2^-,I}}\right)} \frac{S_{\text{NO}_2^-}}{K_{\text{NO}_2^-} + S_{\text{NO}_2^-}} X_{\text{AOB}}$
BOT								$\text{Mred} + \text{Mox} = C_{\text{tot}}$

AOH, ammonia oxidation to hydroxylamine by AOB; HON, hydroxylamine oxidation to nitrite by AOB; NO, nitrite oxidation by NOB; BOT, balance of the total mediate.

was developed to transform current signals, process data, restore and real-time display the results.

The OUR reported in this work was exogenous OUR, which was obtained by subtracting the endogenous OUR from the total measured OUR. The total biomass concentration and concentration of substrates and additions in each respirometric test are presented in Table 2. In all the respirometric tests, the DO concentrations were above 4 mg/L to ensure the two system were in an aerobic phase. Three groups of abiotic control experiments were conducted with three substrates ( $\text{NH}_4^+$ -N 10 mgN/L,  $\text{NO}_2^-$ -N 10 mgN/L and  $\text{NH}_2\text{OH}$  10 mgN/L) via the hybrid respirometer system. As expected, the DO concentration did not change during any of these experiments (constant at  $7.6 \pm 0.1$  mg/L). Since the culture used in this study contains

both AOB and NOB, sodium azide ( $\text{NaN}_3$ ) was added in some tests when only AOB was needed to inhibit the NOB (Chandran & Smets 2000). Biomass concentrations of AOB and NOB ( $X_{\text{AOB}}$ ,  $X_{\text{NOB}}$ ) were determined with the yield coefficient of AOB for ammonia oxidation and NOB for nitrite oxidation as described by Chandran and Smets (Chandran & Smets 2000) (Equations (3) and (4)):

$$X_{\text{AOB}} = X_t \frac{Y_{\text{AOB},\text{NH}_4}}{Y_{\text{AOB},\text{NH}_4} + \frac{Y_{\text{NOB}}}{3}} \quad (3)$$

$$X_{\text{NOB}} = X_t \frac{\frac{Y_{\text{NOB}}}{3}}{Y_{\text{AOB},\text{NH}_4} + \frac{Y_{\text{NOB}}}{3}} \quad (4)$$

**Table 2** | Respirometric experimental conditions

Test number	Substrate	$\text{NaN}_3$ ( $\mu\text{mol/L}$ )	$\text{NH}_2\text{OH}$ (mgN/L)	Total biomass concentration
1	$\text{NO}_2^-$ -N (10 mgN/L)	/	/	$407 \pm 27$ (mgCOD/L)
2	$\text{NH}_2\text{OH}$ (5 mgN/L)	24	/	$327 \pm 13$ (mgCOD/L)
3	$\text{NH}_4^+$ -N (10 mgN/L)	24	/	$665 \pm 39$ (mgCOD/L)
4	$\text{NH}_4^+$ -N (8 mgN/L)	24	0	$303 \pm 15$ (mgCOD/L)
5	$\text{NH}_4^+$ -N (8 mgN/L)	24	1	$329 \pm 14$ (mgCOD/L)
6	$\text{NH}_4^+$ -N (8 mgN/L)	24	2	$332 \pm 23$ (mgCOD/L)
7	$\text{NH}_4^+$ -N (8 mgN/L)	24	3	$326 \pm 34$ (mgCOD/L)
8	$\text{NO}_2^-$ -N (8 mgN/L)	/	0	$495 \pm 23$ (mgCOD/L)
9	$\text{NO}_2^-$ -N (8 mgN/L)	/	1	$527 \pm 18$ (mgCOD/L)
10	$\text{NO}_2^-$ -N (8 mgN/L)	/	2	$535 \pm 9$ (mgCOD/L)
11	$\text{NO}_2^-$ -N (8 mgN/L)	/	3	$563 \pm 10$ (mgCOD/L)

**Table 3** | Parameter values for  $\text{NH}_4^+$  and  $\text{NO}_2^-$  oxidation under  $\text{N}_2\text{H}_4$  addition by respirometry and model simulation

Parameter	Definition	Source	Parameter value (avg $\pm$ SD)
$Y_{\text{AOB},\text{NH}_2\text{OH}}$	Biomass yield coefficient for $\text{NH}_2\text{OH}$ oxidation to $\text{NO}_2^-$ by AOB (mgCOD/mg $\text{NH}_2\text{OH-N}$ )	Calculated	$0.377 \pm 0.0629$
$Y_{\text{AOB},\text{NH}_4}$	Biomass yield coefficient for $\text{NH}_4^+$ oxidation to $\text{NO}_2^-$ by AOB (mgCOD/mg $\text{NH}_4^+\text{-N}$ )	Calculated	$0.112 \pm 0.0233$
$Y_{\text{NOB}}$	Biomass yield coefficient for $\text{NO}_2^-$ oxidation to $\text{NO}_3^-$ by NOB (mgCOD/mg $\text{NO}_2^-\text{-N}$ )	Calculated	$0.224 \pm 0.0168$
$R_{\text{NH}_4^+}$	Specific maximum rate for $\text{NH}_4^+$ oxidation to $\text{NH}_2\text{OH}$ (mmol-N/mgCOD/h)	Estimated	$0.00382 \pm 0.000794$
$R_{\text{NH}_2\text{OH}}$	Specific maximum rate of AOB for $\text{NH}_2\text{OH}$ oxidation to $\text{NO}_2^-$ (mmol-N/mgCOD/h)	Estimated	$0.00151 \pm 0.000252$
$R_{\text{NO}_2^-}$	Specific maximum rate of NOB for $\text{NO}_2^-$ oxidation to $\text{NO}_3^-$ (mmol-N/mgCOD/h)	Estimated	$0.0118 \pm 0.000633$
$K_{\text{NH}_4^+}$	Half-saturation coefficient of $\text{NH}_4^+$ oxidation to $\text{NH}_2\text{OH}$ (mmol-N/L)	Estimated	$0.125 \pm 0.0173$
$K_{\text{Mred}}$	Half-saturation coefficient of Mred for $\text{NH}_4^+$ oxidation to $\text{NH}_2\text{OH}$ (mmol/g-vss)	Ni <i>et al.</i> (2014)	$1 \times 10^{-2} \times C_{\text{tot}}$
$K_{\text{NH}_2\text{OH}}$	Half-saturation coefficient for $\text{NH}_2\text{OH}$ oxidation to $\text{NO}_2^-$ (mg $\text{NH}_2\text{OH-N/L}$ )	Estimated	$0.108 \pm 0.0231$
$K_{\text{Mox}}$	Half-saturation coefficient of Mox for $\text{NH}_2\text{OH}$ oxidation to $\text{NO}_2^-$ (mmol/g-vss)	Ni <i>et al.</i> (2014)	$1 \times 10^{-3} \times C_{\text{tot}}$
$K_{\text{NO}_2^-}$	Half-saturation coefficient for $\text{NO}_2^-$ oxidation to $\text{NO}_3^-$ (mmol-N/L)	Estimated	$0.194 \pm 0.00901$
$K_{\text{NO}_2^-,I}$	$\text{NH}_2\text{OH}$ inhibition coefficient for $\text{NO}_2^-$ oxidation to $\text{NO}_3^-$ (mmol-N/L)	Estimated	$3.233 \pm 0.093$
$K_{\text{NH}_2\text{OH},I}$	Self-inhibition coefficient of $\text{NH}_2\text{OH}$ for $\text{NH}_2\text{OH}$ oxidation to $\text{NO}_2^-$ (mmol-N/L)	Estimated	$1.775 \pm 0.335$
$C_{\text{tot}}$	The sum of Mox and Mred (mmol/g-vss)	Ni <i>et al.</i> (2014)	$10 \times 10^{-3}$

where  $X_{\text{AOB}}$  and  $X_{\text{NOB}}$  is the concentrations of AOB and NOB, respectively,  $X_t$  is the total biomass concentration,  $Y_{\text{AOB},\text{NH}_4}$  is the biomass yield coefficient for  $\text{NH}_4^+$  to  $\text{NO}_2^-$ , and  $Y_{\text{NOB}}$  is the biomass yield coefficient for  $\text{NO}_2^-$  to  $\text{NO}_3^-$ .

### Analytical methods

The samples (10 mL) in the respirometric tests were collected from the aeration chamber after the addition of substrates and at the end of the test using syringes. Consistent with APHA, AWWA and WPCF (APHA *et al.* 1998) protocols,  $\text{NH}_4^+$  and  $\text{NO}_2^-$  were analyzed with colorimetric methods,  $\text{NO}_3^-$  was measured spectrophotometrically. Mixed liquor suspended solids and MLVSS were measured using standard methods (2540) in APHA *et al.* (1998). The hydroxylamine was measured as described by Csaky (Csaky 1948).

## RESULTS AND DISCUSSION

### The yielding coefficient of AOB and NOB

The yield coefficients of AOB for  $\text{NH}_4^+$  to  $\text{NO}_2^-$  oxidation,  $\text{NH}_2\text{OH}$  to  $\text{NO}_2^-$  oxidation and of NOB for  $\text{NO}_2^-$  to  $\text{NO}_3^-$

oxidation were estimated from the difference between the total cumulative oxygen uptake during the respirometric assay and the injected substrate concentrations in tests 1 to 3 (Chandran & Smets 2000). The results of the yield coefficients are listed in Table 3.

The yield coefficients  $Y_{\text{NH}_4}$  in this study is 0.113 mg COD/mg N which is in good agreement with the range of 0.03–0.13 mgVSS/mgN reported by de Kreuk (De Kreuk *et al.* 2007). The value of  $Y_{\text{NH}_2\text{OH}}$  was at a similar level as that reported by Ni (Ni *et al.* 2011). The yield coefficient of NOB ( $Y_{\text{NO}}$ ) obtained in the present study (Table 3) was at a similar level to that reported by Sharma (Sharma & Ahlert 1977) of 0.114 mgCOD/mgN but higher than values in the range of 0.0284–0.0994 mgCOD/mgN reported by Vadivelu (Vadivelu *et al.* 2006).

The difference in the strain and growth conditions which resulted in different energy distributions between the growth and the cell maintenance activities (Vadivelu *et al.* 2006) of AOB and NOB which resulted in the fluctuation of a wide range of the growth yield. When  $\text{NH}_2\text{OH}$  is employed instead of  $\text{NH}_4^+$ , as there is no electron needed for the oxidation of  $\text{NH}_4^+$  to  $\text{NH}_2\text{OH}$ , more electrons are allocated to the anabolism (Hooper 1989). Thus, the value of  $Y_{\text{AOB},\text{NH}_2\text{OH}}$  is greater than that of  $Y_{\text{AOB},\text{NH}_4}$ .

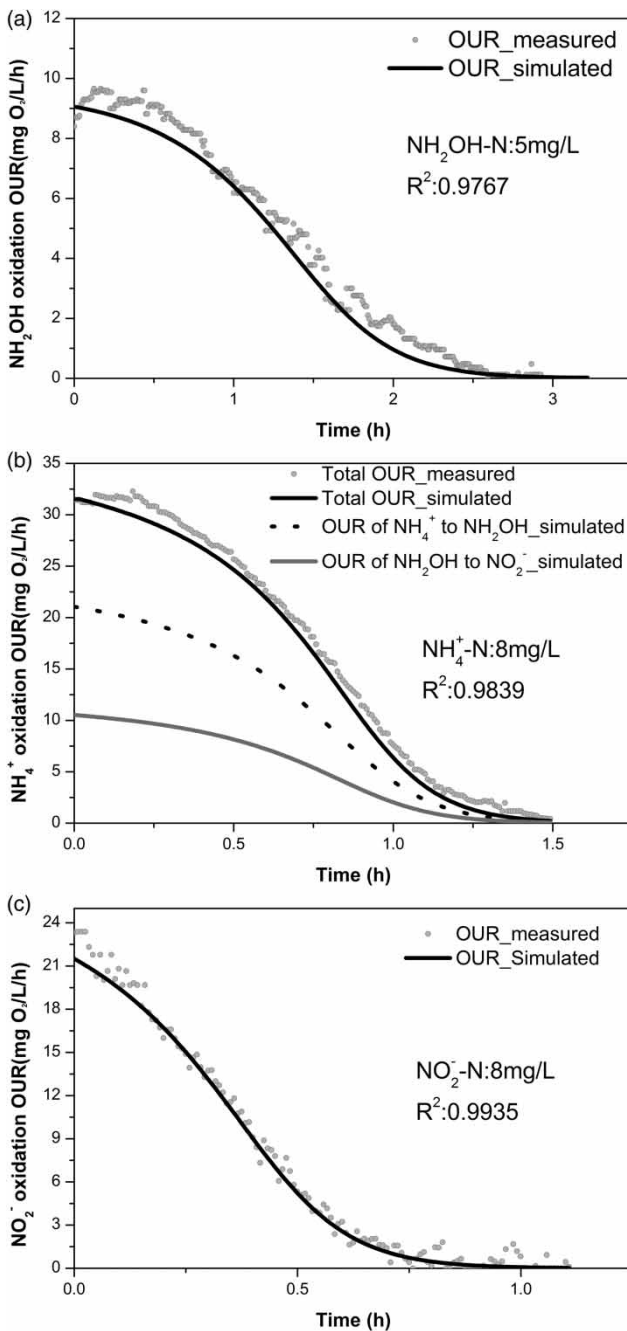


**Figure 1** | Measured and simulated exogenous OUR profiles of  $\text{NH}_2\text{OH}$  oxidation (a),  $\text{NH}_4^+$  (b) oxidation and  $\text{NO}_2^-$  oxidation (c).

### Model calibration and simulation

Figure 1 shows the experimental OUR data of the  $\text{NH}_2\text{OH}$  oxidation,  $\text{NH}_4^+$  oxidation and  $\text{NO}_2^-$  oxidation as well as the model simulated data. The kinetic parameters of the nitrification were evaluated with the OUR profiles obtained in respirometric tests 4 to 11. The calibrated parameter

values giving the optimum model fittings with the experimental data are listed in Table 3.

According to the modeling result in this study, the  $\text{NH}_4^+$ -N half-saturation coefficient of AOB,  $K_{\text{NH}_4^+}$ , is in the range of  $0.0143\text{--}0.428 \text{ mmol NH}_4^+\text{-N/L}$  (Lackner & Smets 2012) which is in good agreement with the result of Ni (Ni *et al.* 2011) and Law (Law *et al.* 2012). The half-saturation coefficient of  $\text{NH}_2\text{OH}$  for AOB,  $K_{\text{NH}_2\text{OH}}$ , is smaller than that reported by Ni (Ni *et al.* 2011), but similar to the value  $0.05 \text{ mmol}$  reported by Law (Law *et al.* 2012). The  $\text{NO}_2^-$ -N half-saturation coefficient of NOB,  $K_{\text{NO}_2^-}$ , estimated in the present study (Table 3), was at a similar level as that reported by Wiesmann (Wiesmann 1994), but appreciably greater than the value at  $0.73 \pm 0.1 \text{ mgNOD/L}$  (i.e.  $0.0457 \pm 0.006 \text{ mmol NO}_2^-\text{-N/L}$ ) reported by Chandran (Chandran & Smets 2000).

The maximum specific ammonia consumption rate for ammonia oxidation to hydroxylamine ( $R_{\text{NH}_4^+}$ ) in the present work was smaller than that reported by Ni (Ni *et al.* 2011). The specific maximum rate of AOB for  $\text{NH}_2\text{OH}$  oxidation to  $\text{NO}_2^-$  ( $R_{\text{NH}_2\text{OH}}$ ) estimated in the present work (Table 3) was a little smaller than the value of  $0.1475 \text{ mmol}/(\text{mgVSS}\cdot\text{h})$  reported by Ni (Ni *et al.* 2011) but was at a similar level to those ( $0.019\text{--}0.092/\text{h}$ ) reported by de Kreuk and Wiesmann (Wiesmann 1994; De Kreuk *et al.* 2007). The specific maximum rate of NOB for  $\text{NO}_2^-$  oxidation ( $R_{\text{NO}_2^-}$ ) in this work (Table 3) was higher than the value reported by Ni (Ni *et al.* 2011).

The reported kinetic parameters for both  $\text{NH}_4^+$  oxidation and  $\text{NO}_2^-$  oxidation is not identical in the reported research. Different wastewater characteristics and reactor operation conditions affecting microbial communities could be related to the difference among the measured kinetic parameters. Such aforementioned differences are associated with temperatures and pH values, which were found to influence the growth or substrate consumption rate of the nitrifiers significantly (Contreras *et al.* 2008). Additionally, the specific growth rate in the sludge could also be related to the different energy requirement of cell maintenance of the sludge.

### The effect of hydroxylamine

To study the effect of hydroxylamine on the AOB and NOB, respectively, the respirometric tests were conducted with the substrates ( $8 \text{ mg/L}$  ammonia and  $8 \text{ mg/L}$  nitrite, respectively) under three different hydroxylamine levels (tests 5 to 7 and tests 9 to 11). Figure 2 displays the measured and simulated exogenous OUR profiles of  $\text{NH}_4^+$  oxidation (Figures 2(a) to (c)) and  $\text{NO}_2^-$  oxidation (Figures 2(d) to (f))

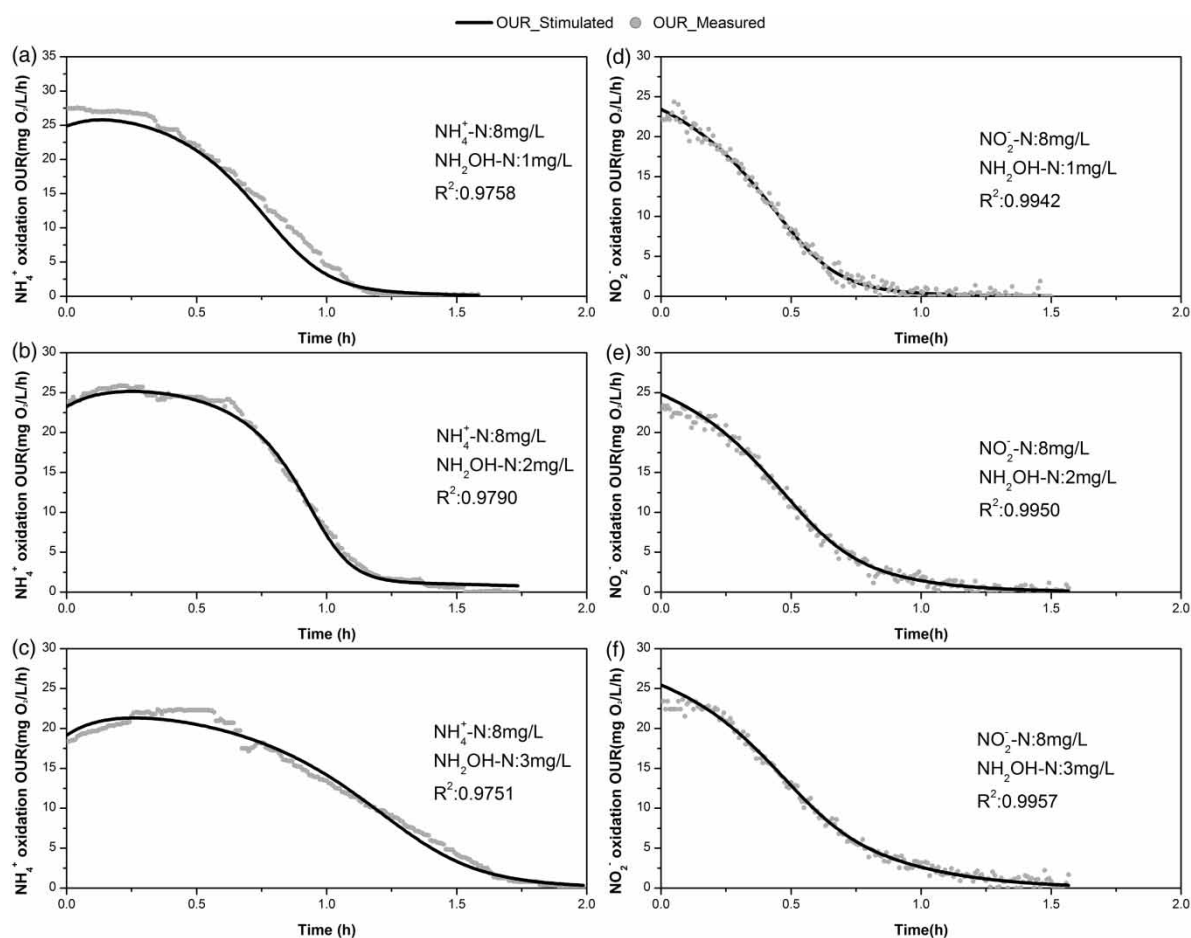


**Figure 2** | Measured and simulated exogenous OUR profiles of  $\text{NH}_4^+$  oxidation and  $\text{NO}_2^-$  under different concentrations of hydroxylamine.

under different concentration level of hydroxylamine. The addition of hydroxylamine has inhibition effects on both ammonia oxidation and nitrite oxidations. The time needed for OUR declining to 0 increased with the improving of the hydroxylamine concentration. This is consistent with the modeling assumption that the inhibition of hydroxylamine has a positive correlation with its concentration.

It has been suggested that hydrazine, a substrate analogue for the hydroxylamine-oxidizing enzyme (Nicholas & Jones 1960), inhibits the oxidation of ammonia as the dehydrogenation of hydrazine competing with that of hydroxylamine (Anderson 1965). It seems that additional hydroxylamine will inhibit the oxidation of hydroxylamine itself, and consequently shrink the electron production that is needed for the AMO to catalyze the oxidation of ammonia. Therefore, the ammonia oxidation is inhibited by the hydroxylamine indirectly.

This study firstly investigated the self-inhibition coefficients for hydroxylamine oxidation ( $K_{\text{NH}_2\text{OH},I}$ ) and

noncompetitive inhibition coefficient for nitrite oxidation ( $K_{\text{NO}_2^-,I}$ ). As shown in Table 3, the value of  $K_{\text{NO}_2^-,I}$  was greater than  $K_{\text{NH}_2\text{OH},I}$ , from which it can be inferred that the inhibitive effect of hydroxylamine on nitrite oxidation was stronger than that on the hydroxylamine oxidation.

## CONCLUSION

The kinetic model of nitrification was established, which isolated hydroxylamine oxidation from ammonia oxidation. The kinetic parameters for  $\text{NH}_4^+$  and  $\text{NO}_2^-$  oxidations under effect of hydroxylamine were obtained by respirometry experiment and model simulation. According to the results, the added hydroxylamine results in the self-inhibition of its oxidation, and indirectly inhibits the oxidation of ammonia. The inhibition of hydroxylamine on nitrite oxidation is noncompetitive. The self-inhibition coefficient of hydroxylamine oxidation is  $1.775 \pm 0.335$  mmolN/L and noncompetitive

inhibition coefficient of nitrite oxidation is  $3.233 \pm 0.093$  mmolN/L. The kinetic parameters are applicable when hydroxylamine concentration is up to 3 mmol/L.

## ACKNOWLEDGEMENTS

The partial financial support from the Scientific Research Foundation (2011DA105287-ZD201505) of State Key Laboratory of Coal Mine Disaster Dynamics and Control, the financial support of the Natural Science Foundation of China (NSF 51078365), the Natural Science Funds of Chongqing under grant (cstc2013jjB20002) and the National Science and Technology Major Project for Water Pollution Control and Remediation (2012ZX07307-001) is gratefully acknowledged.

## REFERENCES

- Anderson, J. H. 1965 Studies on the oxidation of ammonia by nitrosomonas. *Biochem. J.* **95**, 688–698.
- APHA, AWWA and WPCF 1998 *Standard Methods for the Examination of Water and Wastewater*. American Public Health Association, American Water Works Association, Water Pollution Control Federation, Washington, DC, USA.
- Chandran, K. & Smets, B. F. 2000 Single-step nitrification models erroneously describe batch ammonia oxidation profiles when nitrite oxidation becomes rate limiting. *Biotechnol. Bioeng.* **68** (4), 396–406.
- Contreras, E. M., Ruiz, F. & Bertola, N. C. 2008 Kinetic modeling of inhibition of ammonia oxidation by nitrite under low dissolved oxygen conditions. *J. Environ. Eng.* **134** (3), 184–190.
- Csaky, T. 1948 On the estimation of bound hydroxylamine in biological materials. *Acta Chem. Scand.* **2** (5–6), 450–454.
- De Kreuk, M., Picioreanu, C., Hosseini, M., Xavier, J. & Van Loosdrecht, M. 2007 Kinetic model of a granular sludge SBR: influences on nutrient removal. *Biotechnol. Bioeng.* **97** (4), 801–815.
- Harper Jr., W. F., Terada, A., Poly, F., Le Roux, X., Kristensen, K., Mazher, M. & Smets, B. F. 2009 The effect of hydroxylamine on the activity and aggregate structure of autotrophic nitrifying bioreactor cultures. *Biotechnol. Bioeng.* **102** (3), 714–724.
- Henze, M., Gujer, W., Mino, T. & Van Loosdrecht, M. 2006 Activated sludge models ASM1, ASM2, ASM2d and ASM3.
- Hoffman, T. & Lees, H. 1953 The biochemistry of the nitrifying bacteria. *Biochem. J.* **54**, 579–583.
- Hooper, A. 1989 Biochemistry of the nitrifying lithoautotrophic bacteria. In: *Autotrophic Bacteria*, H. G. Schlegel & B. Bowien (eds), Springer-Verlag, Berlin, Germany, pp. 239–281.
- Hooper, A. B., Vannelli, T., Bergmann, D. J. & Arciero, D. M. 1997 Enzymology of the oxidation of ammonia to nitrite by bacteria. *Antonie van Leeuwenhoek* **71** (1–2), 59–67.
- Kampschreur, M. J., Tan, N. C., Kleerebezem, R., Picioreanu, C., Jetten, M. S. & Loosdrecht, M. C. v. 2007 Effect of dynamic process conditions on nitrogen oxides emission from a nitrifying culture. *Environ. Sci. Technol.* **42** (2), 429–435.
- Lackner, S. & Smets, B. F. 2012 Effect of the kinetics of ammonium and nitrite oxidation on nitrification success or failure for different biofilm reactor geometries. *Biochem. Eng. J.* **69**, 123–129.
- Law, Y., Ni, B., Lant, P. & Yuan, Z. 2012 Nitrous oxide (N<sub>2</sub>O) production by an enriched culture of ammonia oxidising bacteria depends on its ammonia oxidation rate. *Water Res.* **46** (10), 3409–3419.
- Ni, B.-J., Rusalleda, M., Pellicer-Nacher, C. & Smets, B. F. 2011 Modeling nitrous oxide production during biological nitrogen removal via nitrification and denitrification: extensions to the general ASM models. *Environ. Sci. Technol.* **45** (18), 7768–7776.
- Ni, B. J., Peng, L., Law, Y., Guo, J. & Yuan, Z. 2014 Modeling of nitrous oxide production by autotrophic ammonia-oxidizing bacteria with multiple production pathways. *Environ. Sci. Technol.* **48** (7), 3916–3924.
- Nicholas, D. & Jones, O. 1960 Oxidation of hydroxylamine in cell-free extracts of *Nitrosomonas europaea*. *Nature* **185**, 512–514.
- Peili, L., Zhang, D., Zhang, X. & Cao, H. 2006 An implementation of the hybrid respirometric measurement principle with more reliable oxygen uptake rate (OUR) measurement. *Water Pract. Technol.* **1** (4). DOI: 10.2166/wpt.2006.074.
- Reichert, P. 1998 *AQUASIM 2.0 - User Manual*. Swiss Federal Institute for Environmental Science and Technology (EAWAG), CH-8600 Dübendorf, Switzerland, 214 pp.
- Sharma, B. & Ahlert, R. 1977 Nitrification and nitrogen removal. *Water Res.* **11** (10), 897–925.
- Vadivelu, V. M., Yuan, Z., Fux, C. & Keller, J. 2006 Stoichiometric and kinetic characterisation of *Nitrobacter* in mixed culture by decoupling the growth and energy generation processes. *Biotechnol. Bioeng.* **94** (6), 1176–1188.
- Wiesmann, U. 1994 Biological nitrogen removal from wastewater. *Adv. Biochem. Eng. Biotechnol.* **51**, 113–153.

First received 17 June 2015; accepted in revised form 30 October 2015. Available online 11 November 2015